

**Chapter 4: Cloning and expression of
metallothionein genes in *Deinococcus
radiodurans* R1**

*If a man will begin with certainties, he shall end in doubts; but if he will be content to begin with doubts
he shall end in certainties- Sir Francis Bacon*

4.1 Introduction

Many metal ions are essential as trace elements but at higher concentrations they become toxic. Heavy metals are difficult to remove from the environment and unlike many other pollutants cannot be chemically or biologically degraded and are ultimately indestructible. Microorganisms could be used to clean up metal contamination by removing metals from contaminated waste by sequestering metals from soils and sediments, or solubilizing metals to facilitate their extraction. Detoxification of metals by the formation of complexes is a strategy used by most eukaryotes (Nies, 1999).

Metallothioneins (MTs) are low molecular weight (6–7 kDa), cysteine-rich proteins found in animals, higher plants, eukaryotic microorganisms and some prokaryotes. They are divided into three different classes on the basis of their cysteine content and structure (Cobbett and Goldsbrough, 2002). The Cys-Cys, Cys-X-Cys and Cys-X-X-Cys motifs (in which X denotes any amino acid) are characteristic and invariant for MTs. The first prokaryotic MT to be identified are from cyanobacterial strains of the genus *Synechococcus* which is encoded by the *smtA* gene, contains fewer cysteine residues than mammalian MTs (Huckle et al., 1993). Deletion of the *smt* locus reduces Zn/Cd tolerance (Turner et al., 1993). The *smt* locus includes *smtA*, which encodes a class II MT (Olafson et al., 1988) and a divergently transcribed gene *smtB* which encodes a repressor of *smtA* transcription (Huckle et al., 1993). SmtA has at least three distinct metal binding sites coordinates to three Zn²⁺ ions via eight Cys residues. Two metal sites contain exclusively Cys-thiolate ligands, whereas the third contains both Cys-thiolate and His- imidazole ligands (Blindauer et al., 2001; Blindauer et al., 2002).

Phytochelatins (PCs) are short, cysteine-rich peptides with the general structure (γ Glu-Cys)_n Gly (n 4–11). PCs offer many advantages over MTs due to their unique structural characteristics, particularly the continuously repeating γ Glu-Cys units. The presence of a γ bond between glutamic acid and cysteine in PCs indicates that these peptides must be synthesized enzymatically. An attractive alternative strategy is to develop organisms harboring synthetic genes encoding protein analogs of PC with the general structure (Glu-Cys)_n Gly (ECs). These peptides differ from PCs because the peptide bond between glutamic acid and cysteine is not the γ bond since synthetic phytochelatin are synthesised by the ribosomal machinery (Malin and Bulow, 2001).

Bae et al., (2000) demonstrated the efficacy of the synthetic phytochelatin in chelating Cd^{2+} .

Radioactive waste sites are a concoction of several hydrocarbons such as trichloroethylene, toluene and xylene apart from the radioactive metals such as uranium, plutonium, cesium and non radioactive heavy metals such as cadmium, mercury, lead and chromium. Due to the prohibitive cost of cleaning up of the nuclear waste, bioremediation is an attractive alternative for the clean up of the nuclear waste sites. However there are certain inherent disadvantages of using *D. radiodurans* R1 (DR1). It has been found that nutrient conditions have a profound effect on the survival and growth of DR1 during chronic exposure to irradiation (Venkateswaran et al., 2000). Ruggiero et al., (2005) have demonstrated that the concentrations of metals that inhibit DR1 growth are lower than the concentration inhibitory to other bacteria.

The fact that DR1 is not extraordinary in its tolerance to metals and proximate radionuclides is not surprising. DR1 can grow while exposed to exceptionally high dose of 6000 rads h^{-1} (60 Gy h^{-1}) γ radiation from an external source. Metal toxicity is generally related to cell penetration and subsequent damage to the cellular machinery (Silver, 1998; Sarkar, 2002) while DR1's radiation resistance is attributed to fast and efficient DNA repair mechanisms (Battista, 1997; Battista et al., 2000; Fredrickson et al., 2000), its radiation resistance is unlikely to correlate with its actinide or heavy metal resistance except in cases where the actinide or the metal directly catalyses DNA damage. The expression of metal reduction or resistance genes or expansion of its metal reduction abilities could augment DR1's functionality (Fredrickson et al., 2000).

Deinococcus strains demonstrate exceptional sensitivity to Cd^{2+} (Ruggiero et al., 2005; this work, Chapter 3). Immobilization by intracellular binding to metallothionein is an attractive alternative to reduce the toxicity of Cd^{2+} and other heavy metals in deinococci. DR1 has been reported to be transformed for varied bioremediative processes (Lange et al., 1998; Brim et al., 2000; Brim et al., 2006; Appukutan et al., 2006). Albeit the success of the recombinant strains at the lab scale their field application has never been demonstrated. Construction of recombinant strains of DR1 that can survive high metal concentrations at the radioactive waste sites and subsequent co-transformation of such strains with metabolic genes for mineralization of toxic hydrocarbon and metal can enhance the applicability of DR1 for bioremediation at the nuclear waste sites. Quin et al., (2006) demonstrated the

expression of Mer R metal binding domain for enhanced metal sequestration in DR1. Considering the bioremediative application of DR1, this work deals with the intracellular expression of metallothioneins (both synthetic and natural) in DR1 to expand the metal tolerance for its better applicability at the nuclear waste sites.

4.2 Material and Methods

4.2.1 Bacterial strains, and Plasmids used in this study

The bacterial strains and plasmids used in this study as described in Table 4.1.

Table 4.1 Strains and Plasmids used in this study

Strain or Plasmid	Relevant information	Source/Ref.
<i>E. coli</i> DH5 α	<i>supE44 DlacU (f80lacZDM15) hsdR17 recA1 endA1 gyrA96 thi 1 relA1</i>	Laboratory stock
<i>E. coli</i> BL-21(DE3)	<i>F-ompT gal(dcm)(lon)hsdS_B(r_B⁻ m_B⁻ an E.coli B strain)with DE3, a λ prophage carrying the T7 polymerase gene</i>	Lab. stock (Sambrook & Russell, 2001)
<i>D. radiodurans</i> R1 ATCC13939	Wild type	Prof. Mary Lidstrom, University of Washington, Seattle, USA.
DR1 (pradZ3)	DR1 harbouring pRADZ3	This study
DR1 (pRAD-EC)	DR1 harbouring pRAD-EC	This study
DR1 (pRAD- smt A)	DR1 harbouring pRAD- <i>smtA</i>	This study
Plasmids		
pTZ57R/T	T-vector for the cloning of PCR products Ap ^r	MBI Fermentas, Germany
pRADZ3	Shuttle vector in <i>E. coli</i> and DR1, <i>lacZ</i> fragment of pMUTIN2mcs, putative R1 <i>groESL</i> promoter, Ap ^r Cm ^r	Prof. Mary Lidstrom, University of Washington, Seattle, USA Meima and Lidstrom, 2000.

The sequence in bold faced, italics represents the recognition site of *Xma*I and *Xba*I in EC1 and EC2 respectively. The under lined region represents the region of overlap. Following primers are used for the amplification of the synthetic gene

Forward Primer ECF:

5'- GCT***ACTAGTAGGAGGACCC***CACATG ACCC GGG AAG AAT GTG AAT GT -3'

Reverse Primer ECR:

5'-TGCCG***TCTAGATTAACCA***-3'

The sequence in bold faced, italics represents the recognition site of *Spe*I and *Xba*I in ECF and ECR respectively the under lined sequence represents the ribosome binding site.

ec20 was synthesized using the PCR based strategy wherein EC1 and EC2 were combined at a concentration of 0.3 ng each in a system of 30 μ l comprising of 3 μ l of 10X reaction buffer, 1 μ l of 10 mM dNTPs and 1.5 u of *Taq* DNA polymerase. The PCR cycling conditions for the synthesis of the *ec20* were initial denaturation at 95 °C for 3min followed by ten cycles each comprising of denaturation at 95 °C for 30s, annealing at 41 °C for 30s and extension at 72 °C for 45 s. After 10 cycles template for PCR amplification were generated. At the end of the 10 cycles ECF and ECR were supplemented at a concentration of 0.3 μ M and the PCR was continued for 30 cycles with the PCR cycles consisting of denaturation of 95°C for 30s, annealing at 46°C for 30s and extension at 72 °C for 45 s with final extension at 72 °C for 10 min.

ec20 was synthesized using the PCR based strategy wherein EC1 and EC2 were combined at a concentration of 0.3 ng each in a system of 30 μ l comprising of 3 μ l of 10X reaction buffer, 1 μ l of 10mM dNTPs and 1.5 u of *Taq* DNA polymerase. The PCR cycling conditions for the synthesis of the *ec20* were initial denaturation at 95°C for 3min followed by ten cycles each comprising of denaturation at 95°C for 30s, annealing at 41°C for 30s and extension at 72 °C for 45 s. This would result in the generation of the double stranded *ec20* molecules by overlap extension of EC1 and EC2 which were to be subsequently used as template for PCR amplification with ECF and ECR. At the end of the 10 cycles ECF and ECR were supplemented at a concentration of 0.3 μ M and the PCR was continued for 30 cycles with the PCR cycles consisting of denaturation of 95 °C for 30 s, annealing at 46 °C for 30 s and extension at 72 °C for 45 s with final extension at 72 °C for 10 min.

4.2.5 PCR Amplification of *smtA*

The *smtA* gene, encoding the metallothionein from *Synechococcus* PCC 7942, was PCR amplified from the plasmid pMHN1.1 using the primers

smtA F : CTACTAGTAGGAGGACCCCACATGACATGACCTCA

smtA R: GTGGATCCACTACAGTTGCAGCCGGTGTG

The sequence in bold faced and italics denote the *Spe*I and *Bam*HI sites in *smtA* F and *smtA* R primers, respectively, while the under-lined sequence is the RBS. An appropriate dilution of pMHN1.1 DNA was combined in a system of 30µl comprising of 3 µl of 10X reaction buffer, 1µl of 10 mM dNTPs , 1.5 u of *Taq* polymerase and 0.3 µM each of the forward and reverse primers. The PCR cycling conditions were: initial denaturation at 95 °C for 3min followed by 30 cycles each comprising of denaturation at 95 °C for 30 s, annealing at 58 °C for 45s and extension at 72 °C for 30 s and a final extension of 72 °C for 10 min. The products of the PCR were analysed on 2 % agarose gel.

4.2.6 DNA manipulations

a) Plasmid extraction

Miniscale plasmid DNA preparations from *E. coli*, restriction digestion and ligation were done by standard protocols described by Sambrook and Russell, (2001). Transformation of *E. coli* strains was done using CaCl₂ method (Sambrook and Russell, 2001)

b) Cloning in T-vector

The PCR products obtained were purified by home- made spin columns (Wang and Rossmann, 1994) and cloned in pT57R/T following manufacturer's (MBI Fermentas, Germany) instructions, and transformed in *E. coli* DH5a using CaCl₂ method (Sambrook and Russell, 2001). The clones were confirmed by digestion with *Eco*RI and *Bam*HI and PCR amplification. The PCR cycling conditions were the same as described earlier.

c) Construction of pRAD-EC

The plasmid from T-vector clone, 6ST was digested with *Spe*I and *Xba*I and the insert was purified. The purified *ec* 20 gene was cloned into the *Spe*I, *Xba*I site of purified and dephosphorylated vector, pRADZ3. The ligated product was transformed in *E. coli* DH5a and selected on 50 µg/ml ampicillin. The clones were confirmed by PCR as described above and the products were analysed on 2 % gel. *Spe*I and *Xba*I

digest of the clones were resolved on 10 % acrylamide gel with subsequent silver staining to confirm the presence of insert.

d) Construction of pRAD- *smtA*

SpeI and *BamHI* digested amplified fragment of *smtA* were cloned in *SpeI* and *BamHI* digested, purified pRADZ4. The ligated product was transformed in *E.coli* DH5 α and selected on 50 μ g/ml ampicillin. The clones were confirmed by PCR as described above and the products were analysed on 2 % gel. *SpeI* and *XbaI* digest of the clones were resolved on 10 % acrylamide gel with subsequent silver staining to confirm the presence of insert.

e) Plasmid transformation in DR1

Transformation of DR1 was performed by the calcium chloride method as described by Satoh et al., (2009). Briefly, DR1 cells (1 ml) grown to early stationary phase (16 h of approx. 1.2 OD_{600 nm}) were harvested by centrifugation, at 9650 g or 3 min, washed with 1 ml of TGY broth, resuspended in 0.1 ml of TGY broth, amended with 40 μ l of 0.3 M CaCl₂. A 30 μ l aliquot of the cell mixture and 10 μ l of plasmid DNA (200–400 μ g per μ l) were mixed in a new culture tube and incubated at 30°C for 90 min. To this was then added 2 ml of TGY broth and the mixture was incubated at 30 °C for 24 h. The culture was appropriately diluted with 10 mM sodium phosphate buffer (pH 7.0), spread on TGY plates supplemented with 3 μ g /ml chloramphenicol. The transformants were scored after 3-5 days of incubation at 30 °C.

4.2.7 Expression analysis of *smt A* in *E.coli* BL21 (DE3)

E. coli BL-21 (DE3) cells harbouring the expression plasmid, pMHR1.1, were grown to an OD₆₀₀ of approximately 0.4 to 0.5. Gene expression was induced by treatment with 1 mM IPTG (isopropyl-1-thio-L-D-galactopyranoside) and cells were further incubated for 3 h at 37 °C. The cells were centrifuged at 9600 g for 3 min to remove the supernatant and washed with Phosphate Buffer Saline (PBS; containing 137mM NaCl, 2.7mM KCl, 10mm Na₂HPO₄ and 2mM KH₂PO₄ pH 7.4). Cells were stored as frozen pellet at -20 °C. Cells were stored as frozen pellets at -20 °C. The thawed cells were disrupted by sonication in 10mM PBS, centrifuged at 12,000 g for 10 min. The supernatant was collected and mixed with 5x gel loading dye, boiled for 2-3 min and analysed on 15 % SDS-PAGE for the expression of recombinant protein with against un-induced cultures. Protein estimation was done using Bradford's protein estimation method (Bradford, 1976)

4.2.8 SDS-PAGE analysis

Proteins were fractionated and analysed on 15 % SDS-PAGE using standard procedures (Sambrook and Russell, 2001).

4.2.9 Cd²⁺ tolerance

Cd²⁺ tolerance of the isolates was examined by D₅₀ determination as explained in Section 3.2.3.

4.2.10 Metal estimation by ICP-AES

50 ml cultures were grown in TGY to saturation in presence or absence of Cd²⁺. The cultures were pelleted at 12,300 g for 5 min and washed twice with saline. The pellet was dried at 60 °C overnight in pre-weighed glass vials. Pelleted cells were digested overnight in 1ml of digesting solution (1:1 mixture of 50 % HNO₃ (v/v) and 30% (w/v) H₂O₂) at 60 °C. The volume was increased to 10 ml with H₂O and filtered through Whatman 3. The metal content was analysed by ICP-AES (Helbig et al., 2008).

4.3 Results and Discussion

An attractive strategy to develop metal resistance in organisms is to clone and express synthetic genes encoding protein analogs of PC with the general structure (Glu-Cys)_n Gly (ECs). These peptides differ from PCs because the peptide bond between glutamic acid and cysteine is the standard α peptide bond that can be synthesized on the ribosomal machinery. Synthetic phytochelatin unlike the metallothionein are synthesised by the ribosomal machinery and contain α peptide bond instead of the γ peptide bond characteristic of the phytochelatin simplifying the expression of synthetic PCs in several host bacteria.

4.3.1 Synthesis, amplification and cloning of synthetic phytochelatin, *ec20*

The oligonucleotides employed for the construction of synthetic phytochelatin consisted of glutamate cysteine repeats, occurring twenty times hence the name *ec20*. The sequence of the oligonucleotide was kept the same as described by Bae et al., (2000). A PCR based approach was adopted for the synthesis of phytochelatin as described in Fig. 4.1. The first round of PCR amplification included annealing of the complementary region of EC1 and EC2 followed by overlap extension by *Taq* DNA polymerase to generate synthetic *ec20* gene which was further amplified by the terminal primers. Fig. 4.2 shows the amplified fragment of the *ec20*. *ec20* was cloned

in the pTZ57R/T and the clones were analysed by *EcoRI* and *HindIII* digestion (Fig. 4.3 A). PCR amplification of the random clone was also carried out (Fig. 4.3 B) to confirm the presence of the clones. Confirmed clone pTZ57RT 6ST (6ST) was employed for further sub-cloning (Fig. 4.4).

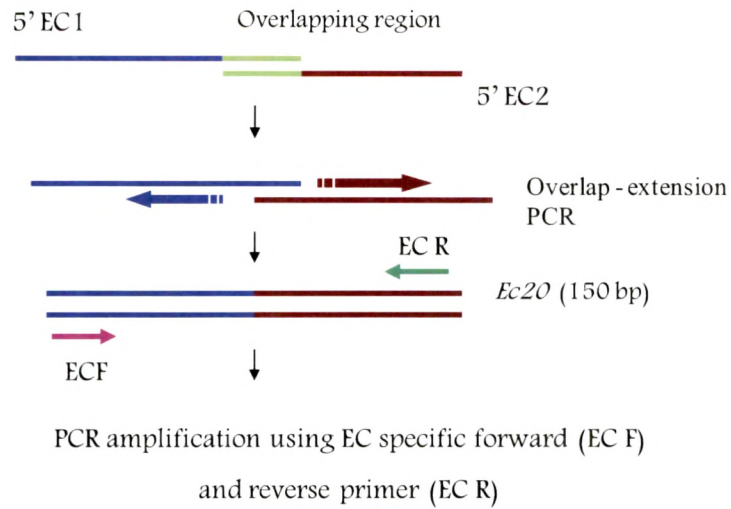


Fig. 4.1 Scheme for synthesis of *ec20*

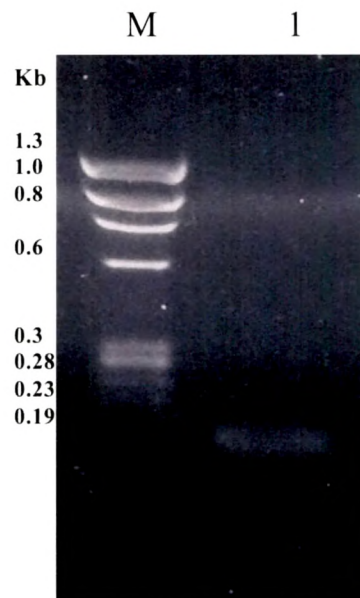


Fig. 4.2 Synthesis and PCR amplification of *ec20*.

M: ϕ X 174 DNA *Hae* III digest marker; 1: amplified *ec20*

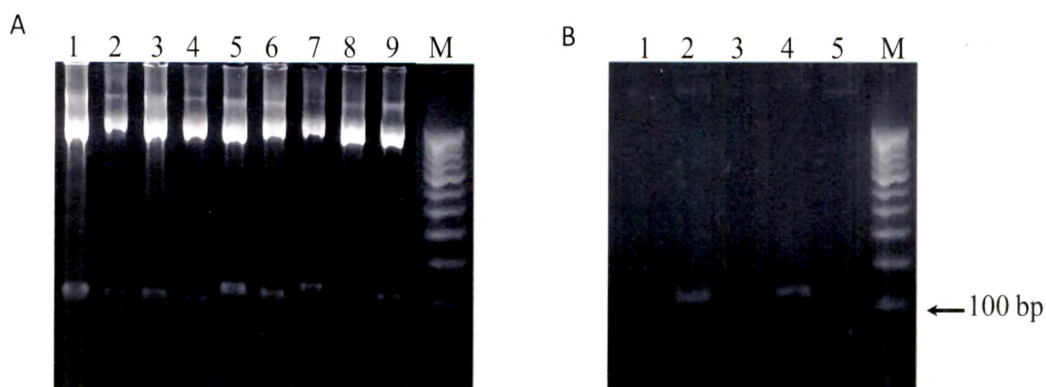


Fig. 4.3 T-vector clone confirmation of *ec-20*.

A) Restriction digestion, *EcoRI* and *XbaI*; Lane 1-9: clones 1-9; M: 100 bp ladder;
 B) PCR amplification Lane 1: Negative control; Lane 2: Clone 6, 6ST; Lane 3: Clone 7,7ST; Lane 4: Clone 13, 13 ST; Lane 5: Clone 1, 1ST; Lane M: 100 bp marker.

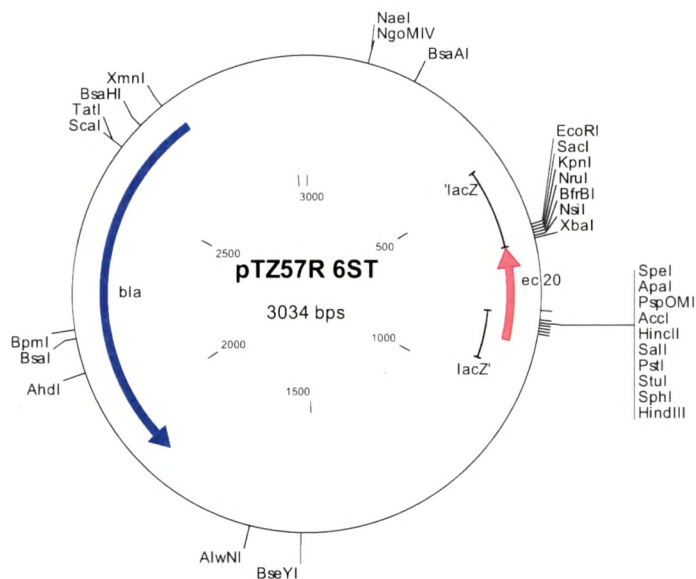


Fig. 4.4 Vector map of pTZ57R-6ST

4.3.2 Sub-cloning of *ec 20* in pRADZ3

For expression of *ec 20* in DR1 pRADZ3 was chosen wherein the *lac Z* is under the effect of PgroEL (Meima and Lidstrom, 2000). Fig. 4.5 depicts the strategy of cloning of *ec20* in pRADZ3 and the representative map of the clones in pRAD-EC. *ec20* was cloned in *Spe I* and *XbaI* site of pRADZ3 and the clones were confirmed using *XhoI* /*Hind III* (Fig. 4.6) and *SpeI* / *XbaI* digestion (Fig. 4.7A). The short listed clones were subsequently confirmed by PCR amplification (Fig. 4.7B).

4.3.3 Construction of pRAD-*smt* A for heterologous expression in DR1

Smt A is a novel MT and its coordination chemistry is of significance in view of the high affinity for Zn^{2+} and the intracellular exclusively handling of Zn^{2+} (Daniel et al., 1998). The efficacy of the *smt* A has been demonstrated for chelating Zn^{2+} and Cd^{2+} . Heterologous expression of *smt*A in DR1 was carried out to compare the efficiency of chelating Cd^{2+} by naturally occurring MT and synthetic MT. Fig. 4.8 shows the amplification of *smt* A from pMHNRI.1. The expected band of approximately 200 bp was obtained.

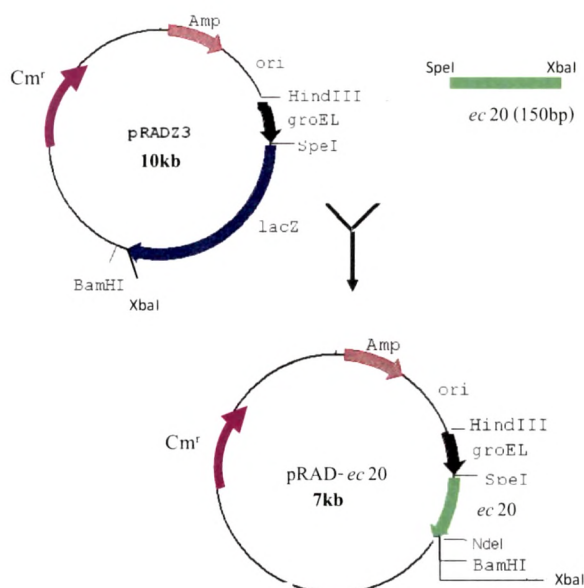


Fig. 4.5 Cloning strategy of *ec20* in pRADZ3 and representative map of pRAD-*EC* clone

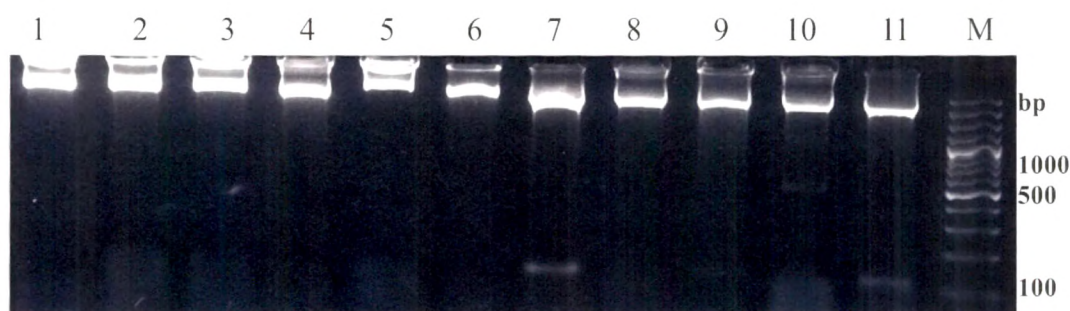


Fig. 4.6 Clone confirmation of *ec20* obtained in pRADZ3 using *Xho*I and *Hind*III of representative clones.

Lane 1: Clone pRAD-1*EC*; Lane2: Clone pRAD-3*EC*; Lane3: Clone pRAD-4*EC*;
Lane4: Clone pRAD-5*EC*; Lane5: Clone pRAD-6*EC*; Lane6: Clone pRAD-7*EC*;

Lane7: Clone pRAD-9EC; Lane8: Clone pRAD-10EC; Lane9: Clone pRAD-11EC;
Lane10: Clone pRAD-12EC; Lane11: Clone pRAD-13EC ; M: 100bp marker

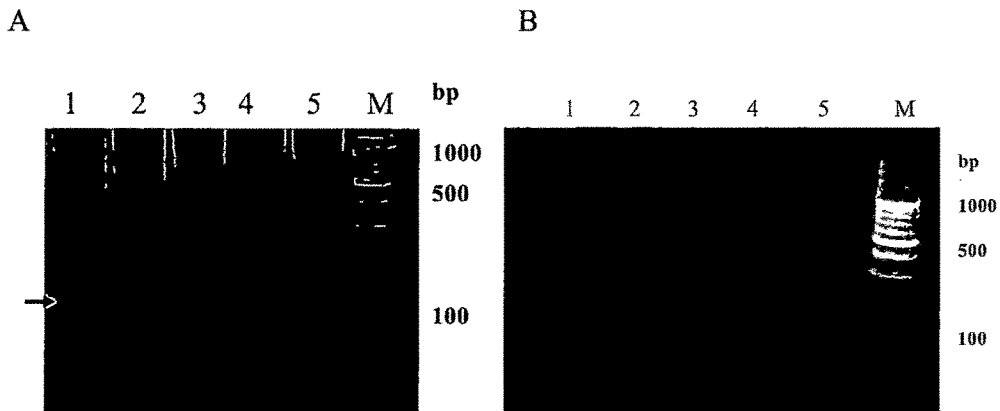


Fig. 4.7 Confirmation of ec 20 clones obtained in pRADZ3. A) using *Spe*I and *Xba*I; B) PCR amplification. Arrow indicates fragment corresponding to *ec* 20. Lanes in Fig.A and Fig.B are listed below.Lane1: Clone pRAD-9EC; Lane2: Clone pRAD-11EC; Lane3: Clone pRAD-13EC; Lane 4: Clone pRAD-14EC; Lane 5: Clone pRAD-18EC.

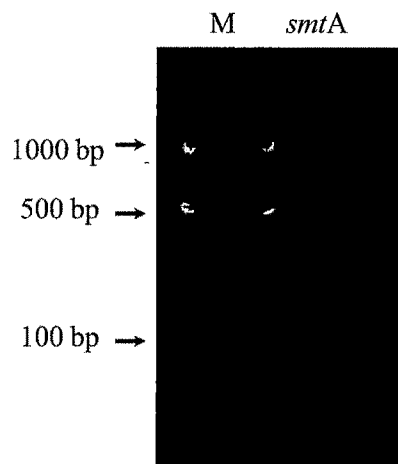


Fig. 4.8 PCR amplification of *smt* A from pMHN1.1.M denotes 100 bp ladder.

pRADZ3 was digested with *Spe* I and *Bam*H I to release lac Z fragment of 3.2Kb. The linearised vector was purified and *smt* A was cloned in the *Spe*I, *Bam*HI site of pRADZ3. Fig. 4.9 depicts the strategy employed for cloning *smt*A in pRADZ3 and the vector map for the ensuing pRAD-*smt* A clones. The clones were randomly selected and confirmed using insert specific enzymes *Spe* I and *Bam*HI to confirm the orientation of the insert (Fig. 4.10) and subsequent confirmation was done using PCR amplification (Fig. 4.11).

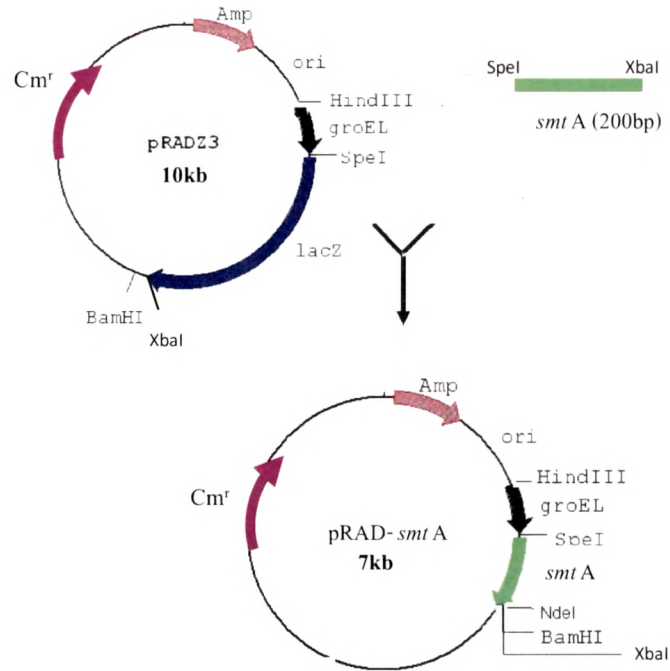


Fig. 4.9 Strategy employed for cloning *smt A* and representative map for the pRAD-*smtA* clones

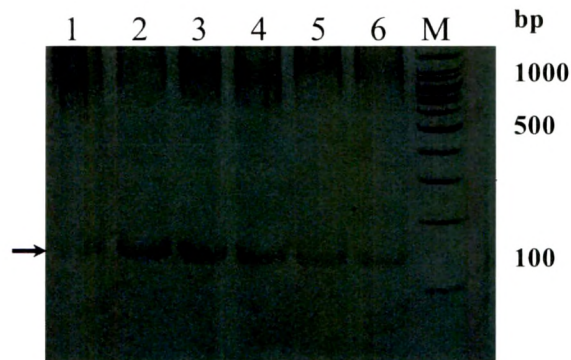


Fig. 4.10 Clone confirmation of pRAD-*smtA* using *Spe I* and *BamHI*. Lane1: pRAD-13 *smtA*; Lane 2: pRAD-18 *smtA*; Lane 3: pRAD-19 *smtA*; Lane 4: pRAD-22 *smtA*; Lane5: pRAD-23 *smtA*; Lane6: pRAD-24 *smtA* ; M: 100bp ladder

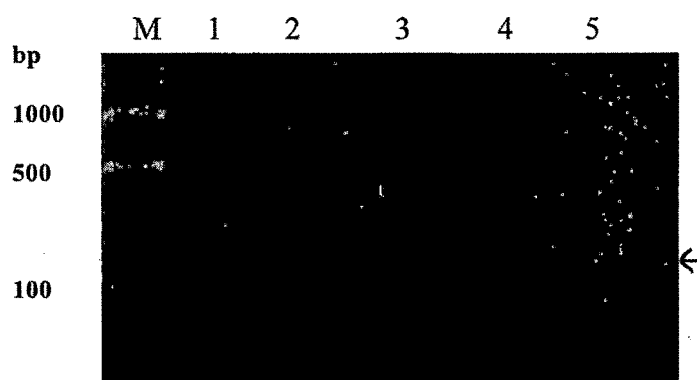


Fig. 4.11 Clone confirmation of pRAD-*smtA* by PCR Amplification.

Lane1: pRAD-13 *smtA*; Lane 2: pRAD-18 *smtA*; Lane 3: pRAD-19 *smtA*; Lane 4: pRAD-22 *smtA*; Lane5: pRAD-23 *smtA*; M: 100 bp ladder

4.3.4 Transformation and expression analysis of pRAD-EC and pRAD-*smtA* in DR1

The plasmid DNA from confirmed clones was transformed in DR1 individually to generate DR1 (pRAD-EC) and DR1 (pRAD-*smtA*). SDS-PAGE analysis of the transformants showed an expected band of 4.5Kda for both DR1 (pRAD-EC) and DR1 (pRAD-*smtA*) (Fig. 4.12). *E. coli* BL-21 (DE3) carrying pMHN1.1, was utilised as a positive control. Although the reported size of SmtA is 5.6 kDa (Blindauer et. al., 2001) a single induced band of > 4.5 kDa in the induced cultures of pMHN1.1, not detectable in the control uninduced plasmid, was observed. From the translated sequence analysis of *ec20*, it has 32 aa which corresponds to expected molecular weight of 3.5 kDa. The observed molecular weight is in agreement with the expected molecular weight of the expressed protein (Fig. 4.12).

4.3.5 Characterization DR1 (pRAD-EC) and DR1 (pRAD-*smtA*)

In pRAD EC and pRAD *smtA* the respective genes are under the influence of the *groESL* promoter. Schimid and Lidstrom, (2002) demonstrated that activity of the promoter *groESL*, as assayed by *lacZ* assay, was not significantly affected at 40 °C and the activity was similar to that determined by 30 °C. However, Holland et al., (2006) demonstrated that best expression from *groES* was obtained at 37 °C. Therefore all further experiments were carried out 37 °C. The growth kinetics was analysed for the vector control and transformants at 37 °C. The expression of *ec20* and *smtA* only slightly enhanced the growth of DR1 at 37 °C (Fig. 4.13).

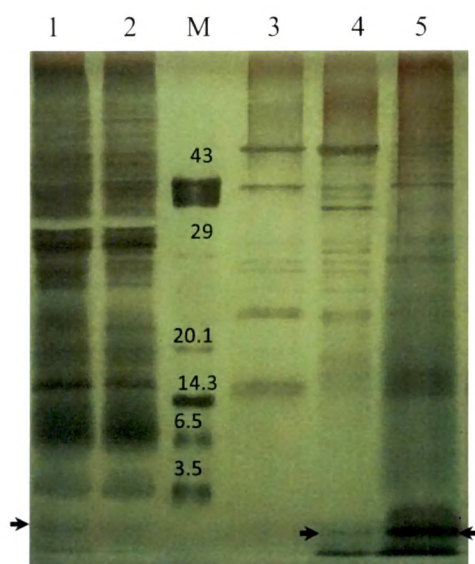


Fig. 4.12 Expression analysis of the DR1 transformants carrying MT. The numbers in the M lane indicate molecular weight in kDa. Lane1: *E.coli* (pMHNr1.1) induced; Lane2: *E.coli* pMHNr1.1 uninduced; Lane M: Low range molecular weight marker; Lane 3: DR1-pRADZ3 vector control; Lane 4: DR1-pRAD EC; Lane 5: DR1-pRAD smtA). The expressed bands are indicated by arrows.

4.3.5a Cd²⁺ tolerance of DR1 (pRAD-EC) and DR1 (pRAD-smtA)

The most important functions of MTs in biological systems are their ability to chelate heavy metals. In most animal and plant cells they are particularly upregulated in presence of Cd²⁺. The capacity of the transformants to tolerate the Cd²⁺ stress was analysed. At the concentrations analysed, the enhanced growth of DR1 (pRAD-EC) indicate the improved capacity to chelate Cd²⁺. The natural MT, *smtA* clone was comparable to the synthetic MT. However at concentrations >10µM no significant effect on survival was observed (Fig. 4.14).

4.3.5b Bioaccumulation of Cd²⁺ by DR1 (pRAD-EC) and DR1 (pRAD-smtA)

The expected outcome of the cloning *ec20* and *smt A* was to sequester Cd²⁺ in DR1 and to improve its survivability in presence of Cd²⁺. Hence the metal sequestration with respect to Cd²⁺ of the transformants was examined. Fig. 4.15 demonstrates Cd²⁺ accumulation by DR1 (pRAD-EC) and DR1 (pRAD-smtA). As compared to vector control, both MT expressing strain accumulated greater Cd²⁺. *smtA* expressing strains, DR1 (pRAD-smtA), accumulated significantly higher amount of Cd²⁺ as opposed to the DR1 (pRAD-EC), expressing synthetic phytochelatin, *ec 20*,. Intracellular levels

of Cd^{2+} in DR1 (pRAD-smtA) were 300 % higher than the control while DR1 (pRAD-EC) accumulated 121 % higher than the control

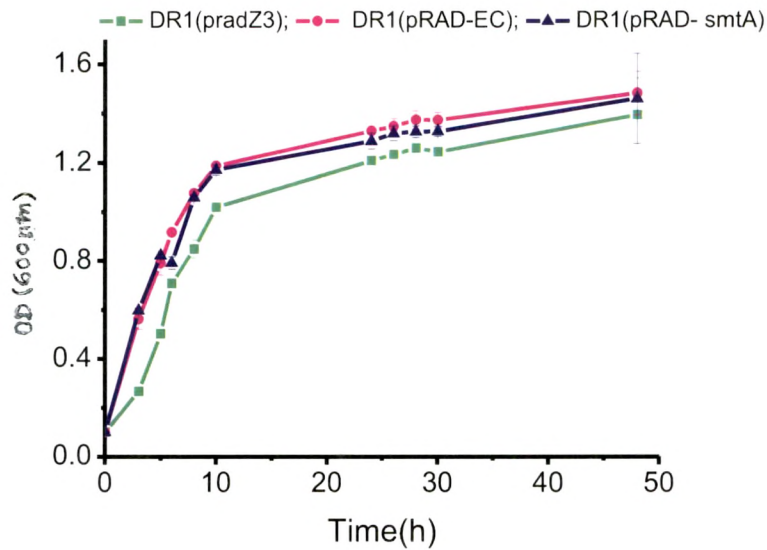


Fig. 4.13 Growth kinetics of DR1 (pRAD-EC) and DR1 (pRAD- *smtA*)

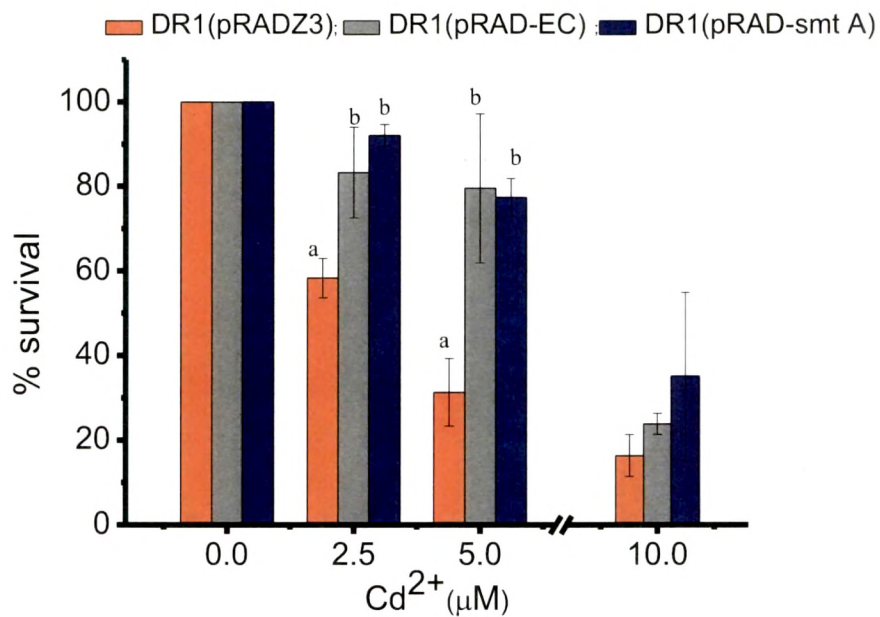


Fig. 4.14 Cd^{2+} tolerance of MT expressing transformants of DR1. Fisher-LSD was carried out determine the significant difference in metal accumulation. Bars with similar alphabet do not differ significantly (LSD test $p < 0.007$)

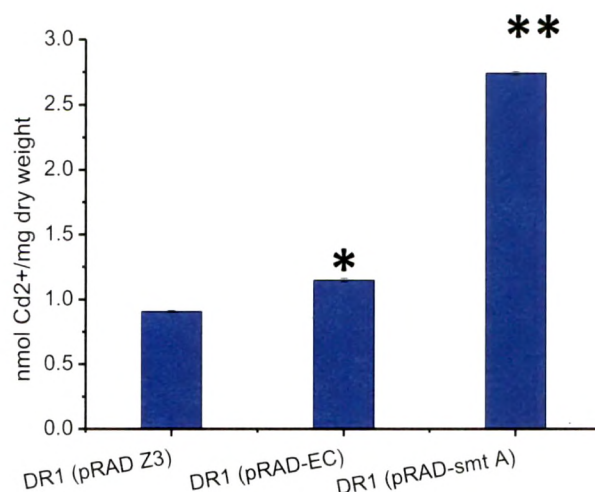


Fig. 4.15 Bioaccumulation of Cd²⁺ by MT transformants of DR1. Fisher-LSD was carried out to determine the significant difference in metal accumulation. $P < 0.03$ is indicated by a single asterisk, while $P < 0.001$ is indicated by a double asterisk.

DR1 demonstrated an enhanced accumulation of Cd²⁺ when synthetic phytochelatin was expressed intracellularly, however, as opposed to the cytoplasmic expression of synthetic phytochelatin in *E. coli* (Pazirandeh et al., 1995), DR1 accumulated 6 fold lesser amount of Cd²⁺. Most of the reports of the synthetic phytochelatin are either displayed on the surface or periplasmically in bacteria and are capable of enhanced chelation of the Cd²⁺ and cellular deposition of Cd²⁺ (Bae et al., 2002; Bae et al., 2000; Xu and Lee, 1999; Veils et al., 1998) (Table 4.2). Bae et al., (2002) reported enhanced accumulation of Cd²⁺ when the phytochelatin was expressed as a fusion to ice nucleation protein of *Pseudomonas* sp. as opposed to periplasmic expression of the same. The intracellularly expressed metallothionein chelates less heavy metal as opposed to expression of the same MT in the periplasmic space, which was attributed to enhanced oxidative stress produced that can oxidise the MT, releasing the bound heavy metal, exacerbating the ROS in the cell (Achard-Joris et al., 2007).

Table 4.2 Metal binding proteins and peptides and their effect on Cd²⁺ accumulation

Peptide/Protein	Expression site	Effect	Ref.
^a His6, single or tandem expressed	OM, LamB	Five- and 11 fold increase in Cd ²⁺ accumulation	Sousa et al., (1996)
^a Human MT	OM, Lpp	66-fold increase in Cd ²⁺ accumulation	Jacobs et al., (1989)
^a Mammalian MT	OM, LamB	15–20 fold increase in Cd ²⁺ accumulation	Sousa et al., (1998)
^a CdBP (HSQKVF)	OM, OmpA	Increased Cd ²⁺ tolerance	Mejare et al., (1998)
^a CP (GCGCPGCG)	OM, LamB	Fourfold increase in Cd ²⁺ accumulation	Pazirandeh et al., (1998)
^a HP (GHHPHG) ₂	OM, LamB	Threefold increase in Cd ²⁺ accumulation	Kotrba, et al. (1999)
^a MT α-domain	OM, LamB	17 fold increase in Cd ²⁺ accumulation	Kotrba et al., (1999)
^a 1-12 tandem repeats of protein <i>Neurospora crassa</i> MT (CGCCG)	Periplasm, maltose binding	10–65 fold increase in Cd ²⁺ accumulation	Mauro and Pazirandeh, (2000)
^a EC(20), synthetic phytochelatin, (Glu-Cys) ₂₀ Gly	OM, Lpp	30 fold increase in Cd ²⁺ accumulation	Bae et al., (2000)
^b Mer R, MBD	Cytoplasmic	Increased tolerance to Hg ²⁺	Quin et al., (2006)
^b EC(20), synthetic phytochelatin, (Glu-Cys) ₂₀	Cytoplasmic	1.21 fold increase in Cd ²⁺ accumulation	This study
^b Prokaryotic MT, Smt A	Cytoplasmic	3 fold increase in Cd ²⁺ accumulation	This study

Abbreviations: OM, outer membrane; LamB, Calcium-binding; Lpp, protein; OmpA, CP, cysteine-containing peptide; HP, histidine-containing; MBD: Metal binding domain peptide.

^a Expression in *E. coli*; ^b Expressed in DR1

4.3.5c Effect of exogenous cysteine on the recombinant strain

SmtA contains a smaller proportion of Cys than synthetic MT (16 % vs. 50 % of residues), and, unlike synthetic MTs, contains His residues, which have been implicated in metal coordination. (Blindauer et al., 2001). Lesser bioaccumulation in synthetic MT was observed which might be as result of the higher cysteine requirement of the cells for synthesising MT. As a result of the binding of Cd^{2+} to sulfide, generated during the biosynthesis of cysteine and of iron-sulfur centers (FeS centers); binding to thiol groups, e.g., of proteins; and the replacement of other transition-metal cations from such sulfur-rich complex compounds (Helbig et al., 2008), the requirement of cysteine may be aggravated in the cells expressing MT in presence of Cd^{2+} . It was hypothesized that the addition of cysteine would relieve the metabolic load and restores the cells capacity to produce MT. Cysteine when added to a final concentration of 0.4 mM, showed an enhanced growth of the transformants as opposed to the vector control (Fig. 4.16). Addition of cysteine at higher concentrations resulted in toxicity to the vector control cells as compared to the transformants which were able to show growth up to 10 μ M. DR1 (pRAD-*smtA*) was able to tolerate greater Cd^{2+} as compared to the DR1(pRAD-EC) similar to that observed for TGY. When compared to growth in TGY, exogenous cysteine boosted the growth by 1.5 fold for vector control as well as for both the transformant. Cysteine amendment rescued Cd^{2+} toxicity for DR1-*smt* at all concentrations and the tolerance to Cd^{2+} at 10 μ M comparable to that of TGY. The growth of DR1-EC and control was retarded in presence of cysteine and Cd^{2+} (Fig. 4.17). Bioaccumulation of Cd^{2+} was determined for the transformants as well as the vector control. Fig. 4.18 illustrates the Cd^{2+} content of the MT expressing strains.

Exogenous cysteine didn't improve the Cd^{2+} sequestration, on the contrary the DR1(pRAD-EC) accumulated least Cd^{2+} , accumulating only 65 % of the control while vector control and DR1(pRAD-*smt A*) accumulated comparable amount of Cd^{2+} . The vector control accumulated less Cd^{2+} in presence of the cysteine as opposed to the same when grown in TGY only. A possible explanation of the reduced Cd^{2+} accumulation could be extracellular chelation of Cd^{2+} by cysteine (Singh and Pandey, 1981) and hence enhanced growth in presence of Cd^{2+} . Reduced accumulation of synthetic MT could not be explained.

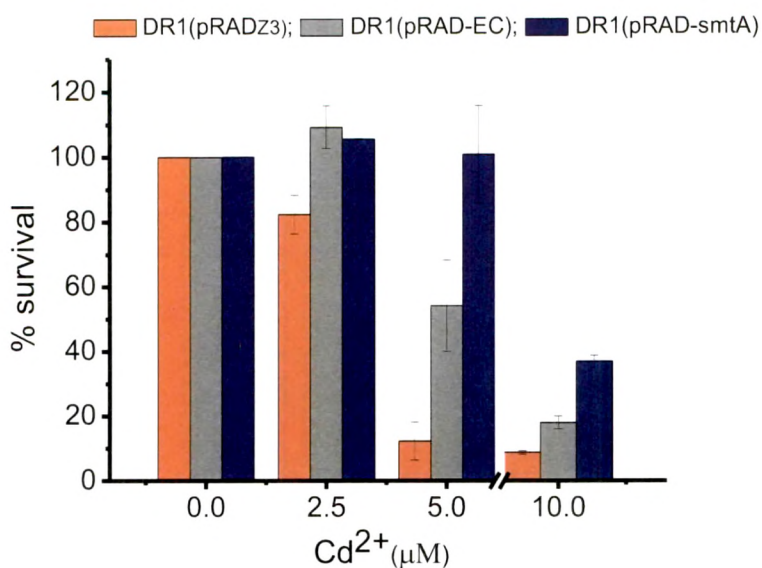


Fig. 4.16 Effect of cysteine on Cd²⁺ tolerance on MT expressing transformants of DR1.

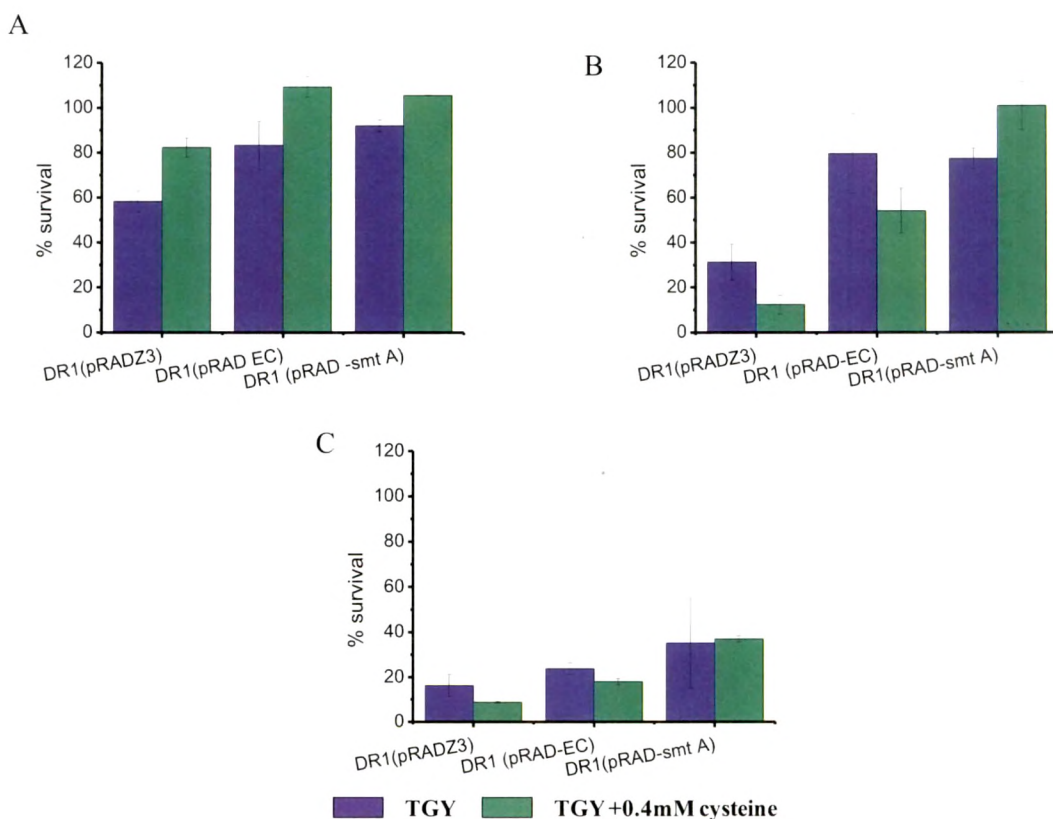


Fig. 4.17: Cd²⁺ tolerance of DR1 expressing MT in presence and absence of 0.4 mM cysteine A) 2.5 μM Cd²⁺; B) 5.0 μM Cd²⁺; C) 10.0 μM Cd²⁺;

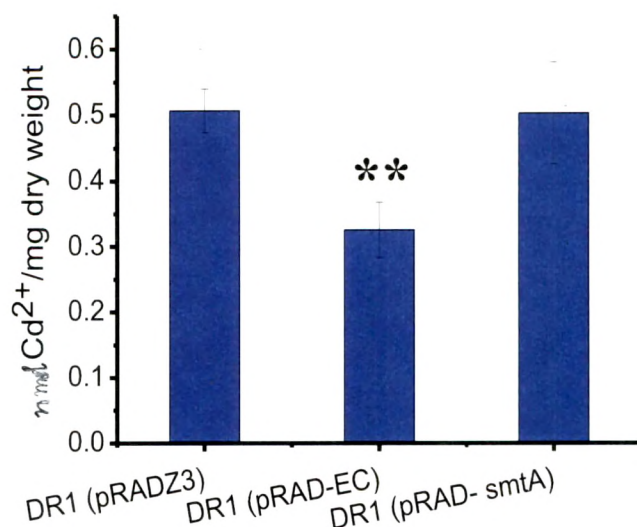


Fig. 4.18 Bioaccumulation of Cd²⁺ by MT transformants of DR1 in presence of cysteine. Fisher-LSD was carried out to determine the significant difference in metal accumulation. P < 0.007 is indicated.

Holland et al., (2006) demonstrated that methionine synthesis proceeds via the B₁₂-dependent enzyme, methionine synthase (MetH, DR0966), rather than the B₁₂-independent MetE and has an incomplete vitamin B₁₂ pathway making the wild type DR1 an auxotroph for methionine. Therefore, reduced intracellular Cd²⁺ by EC 20 expressing strains was attributed to the enhanced metabolic load due to increased cysteine demand in DR1. There is an expected competition for the homocysteine pool for the conversion to methionine and cysteine during Cd²⁺ toxicity as indicated in Fig. 4.19.

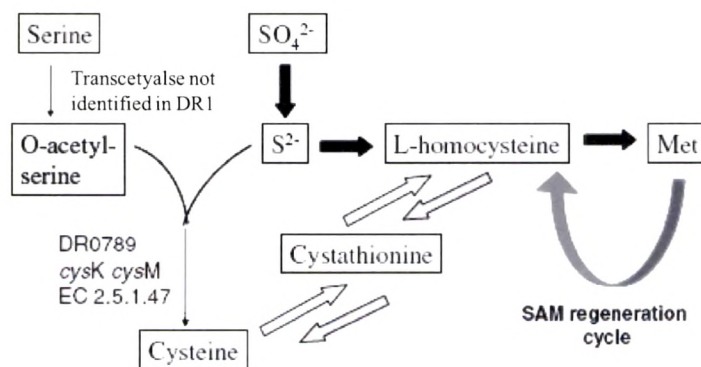


Fig. 4.19 Sulfur recycling in DR1. Black arrows indicate the pathway identified in DR1. (Holland et al., 2006)

4.4 Conclusion

This chapter deals with the expression of synthetic phytochelatin *ec20* as well as natural prokaryotic metallothionein *smt A* in DR1. Qin et al., (2006) reported the cloning of metal binding domain of Mer R and intercellular expression of the same in DR1 which allowed better survival of the transformants in presence of Hg^{2+} . The synthetic phytochelatin was constructed using overlap extension PCR and its subsequent expression in DR1 conferred the transformant, DR1(pRAD-EC), 1.5 fold higher tolerance to Cd^{2+} . DR1(pRAD-EC) accumulated 1.21 fold greater Cd^{2+} as opposed to the control. Heterologous expression of natural metallothionein, *smt A*, in DR1 imparted the transformant, DR1 (pRAD-*smtA*), superior tolerance to Cd^{2+} wherein DR1 (pRAD-*smtA*), amassed 2.5 fold greater Cd^{2+} than DR1-EC. Addition of cysteine enhanced the growth of the DR1 strains harbouring the metallothionein however it did not translate into efficient metal accumulation. The cysteine content of MTs is very high, which might interfere with cellular redox pathways in the cytosol (Raina and Missakis, 1997; Park and Imaly, 2003) may explain the observation.

Intracellular expression of MTs is, however, not devoid of complications and in many instances there have been problems with the stability and short half-life of the expressed heterologous proteins. Expressing MTs fused to a surface protein in DR1 can prove to be an attractive strategy for enhanced bioaccumulation of heavy metals including Hg^{2+} , Cu^{2+} and possibly other thiol-interacting metals.